

## Tunneling spectroscopy of a ballistic quantum wire

A. Ramamoorthy,<sup>1</sup> L. Mourokh,<sup>2</sup> J. L. Reno,<sup>3</sup> and J. P. Bird<sup>4</sup>

<sup>1</sup>Nanostructures Research Group, Department of Electrical Engineering, Arizona State University, Tempe, Arizona 85287-5706, USA

<sup>2</sup>Department of Physics, Queens College of CUNY, 65-30 Kissena Boulevard, Flushing, New York 11367, USA

<sup>3</sup>CINT Science Department, Sandia National Laboratories, P.O. Box 5800, Albuquerque, New Mexico 87185-1303, USA

<sup>4</sup>Department of Electrical Engineering, University at Buffalo, Buffalo, New York 14260, USA

(Received 3 April 2008; revised manuscript received 19 June 2008; published 30 July 2008)

We implement a tunneling-spectroscopy experiment on a ballistic quantum wire by modifying the split-gate method to realize a wire in which an external reservoir can be used to inject tunneling electrons into its interior. We observe a number of features in the tunnel signal of these structures, including a pronounced response associated with the one-dimensional density of states of the wire, as well as signatures of coherent interference of the injected electrons, and dephasing introduced by tunneling of electrons between the wire and the external reservoir.

DOI: [10.1103/PhysRevB.78.035335](https://doi.org/10.1103/PhysRevB.78.035335)

PACS number(s): 73.23.Ad, 73.63.Nm, 73.40.Gk

Tunneling spectroscopy is a powerful tool for the characterization of electronic materials, with a long history of use in the study of superconductors.<sup>1</sup> In low-dimensional semiconductors, it has been applied, to list but a few examples, to study impurity states in two-dimensional electron-gas (2DEG) systems<sup>2,3</sup> and to characterize the density of states (DoS) (Refs. 4–6) and many-body excitations<sup>7</sup> of quasi-one-dimensional (quasi-1D) quantum wires (QWs). In this paper, we apply this method to probe the 1D DoS of a ballistic QW as the strength of its confining potential is varied. The wire is realized by a modification of the split-gate technique<sup>8</sup> that allows us to inject electrons into its interior from a third reservoir, separate from the source and drain [Figs. 1(a) and 1(b)]. With current injected from this “external” reservoir, the voltage drop between the source and drain serves as a detector of this injection and, therefore, of the QW DoS. Using this approach, we investigate the variation of the tunnel signal as the QW is tuned from the situation where several subbands carry its current to that where it is pinched off. The main features in the tunnel signal are found to be due to the enhancement of the 1D DoS that occurs each time a specific subband is driven through the Fermi level.<sup>4</sup> In addition, we also observe quasiregular oscillations of the tunnel signal over a wide range of the QW gate voltage, the characteristics of which are consistent with a Fabry-Pérot interference of electron partial waves in the QW. Finally, we find that, due to the coupling of the QW to the external reservoir, its conductance plateaus<sup>8</sup> are suppressed below the expected integer values of  $2e^2/h$ . This result is explained by considering the consequences of the tunnel coupling of the QW to the external reservoir.

Figures 1(a) and 1(b) show one of our split-gate devices, which was formed in a GaAs/AlGaAs quantum well,<sup>9–11</sup>  $\sim 200$  nm below the top surface (Sandia sample EA739). The 2DEG carrier density, mobility, and mean-free path at 4.2 K were  $2.7 \times 10^{11}$  cm<sup>-2</sup>,  $4 \times 10^6$  cm<sup>2</sup>/V s, and  $\sim 35$   $\mu$ m, respectively. To realize a QW, we applied sufficient depleting voltages to the horizontal “side” gate ( $V_{SG}$ ) and the two vertical “finger” gates ( $V_F$ ), thereby forming a wire approximately 1  $\mu$ m long on the right-hand side. (This procedure could be reversed, forming the QW on the left-hand side of the structure, and the behavior reported here

was also reproduced for this configuration.) With the side gate on the left grounded (Gnd), we then used appropriate Ohmic contacts to make two separate measurements of the device. In the first of these [Fig. 1(a)], we used a four-terminal configuration to determine the QW conductance ( $G_{QW}$ ), while fixed voltage was applied to the side gate ( $V_{SG}$ ) but that applied to the finger gates ( $V_F$ ) was varied. In this setup, an ac voltage of rms magnitude  $V_{in} \geq 100$   $\mu$ V was applied to the probe indicated in Fig. 1(a), driving a current ( $I$ ) through the QW to ground (while the contacts indicated by dotted lines were left floating), allowing the conductance to be determined as  $G_{QW} = (V_1 - V_2)/I$ . The second measurement [Fig. 1(b)] was performed for the same gate conditions as employed in Fig. 1(a), although in this case  $V_{in}$  was applied between the 2DEG on the left (we shall refer to this as the “external reservoir”) and the ground terminal on the QW side (with all contacts indicated by dotted lines again left floating). The resulting voltage drop ( $V_{QW} \equiv V_1 - V_2$ ) across the QW was then monitored as  $V_F$  was varied. Since the QW’s source and drain are unbiased in this configuration,  $V_{QW}$  should be equal to zero in the absence of tunneling. A nonzero  $V_{QW}$  will result, however, if a current flows through the wire as a result of tunneling from the external reservoir.<sup>11</sup> We report detailed measurements here of a single device, although similar behavior to that which we present here was also found in other devices. All measurements were made in a dilution refrigerator with low-frequency ( $\sim 11$  Hz) lock-in detection.

Figure 1(c) captures the main features of our experiment. The right axis plots  $G_{QW}(V_F)$  and shows a steplike variation, indicative of 1D ballistic transport, although the steps are not as well developed as those in other experiments.<sup>8</sup> Büttiker<sup>12</sup> showed that the visibility of the steps is directly related to the shape of the QW confining potential, and Raichev and Debray<sup>13</sup> analyzed this problem extensively. The latter authors indicated that the visibility of the quantized steps increases with decrease in the split-gate separation ( $w$ ) and of the distance between the gates ( $d$ ) and the 2DEG. In our device, however, both of these parameters are relatively large ( $w \sim 350$  nm,  $d \sim 200$  nm). Also present in Fig. 1(c) is a 0.7 feature<sup>14,15</sup> that appears as a point of inflexion, rather than a well-defined plateau, on the transition of  $G_{QW}$  from

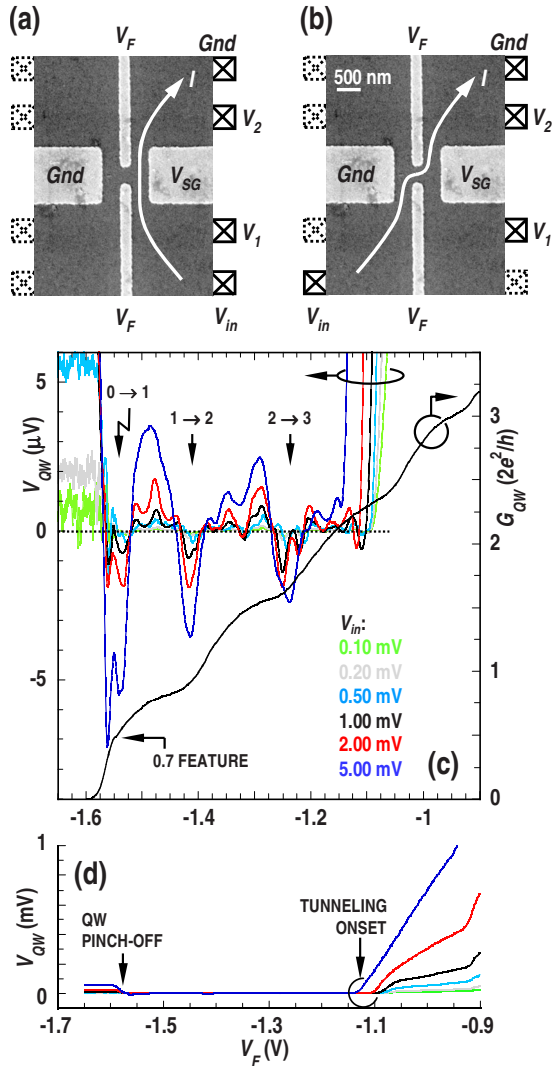


FIG. 1. (Color online) Electron micrographs (gray regions: split gates) showing setup used to measure (a) the conductance of the QW and (b) the voltage drop across the QW due to tunneling from the external reservoir. Contacts indicated by dotted lines are floating in the measurements. (c) The left axis shows  $V_{QW}(V_F)$  for various  $V_{in}$  ( $V_{in}$  indicated,  $V_{SG} = -0.92$  V), while the right axis shows  $G_{QW}(V_F)$  ( $V_{in} = 500$   $\mu$ V). The markers  $0 \rightarrow 1$ ,  $1 \rightarrow 2$ , and  $2 \rightarrow 3$  denote transitions of  $G_{QW}$  to the first, second, and third conductance steps, respectively. (d) Data of Fig. 1(c) are replotted over a larger range of  $V_{QW}$ . Temperature in (c) and (d) is 0.03 K.

the last step to pinch-off. This behavior is actually consistent with other reports in the literature, which show that the 0.7 feature becomes more pronounced when the 2DEG density is lowered below  $2 \times 10^{11}$   $\text{cm}^{-2}$ ,<sup>16</sup> which should be contrasted with our 2DEG density of  $2.7 \times 10^{11}$   $\text{cm}^{-2}$ .

In order to utilize the external reservoir for tunnel spectroscopy, we require that the combined effect of  $V_F$  and  $V_{SG}$  should be such that the constriction formed by the finger gates is pinched off, while the QW itself remains conducting. For fixed  $V_{SG}$ , this defines a specific working range of  $V_F$  as we illustrate in Fig. 1(d). This plots  $V_{QW}(V_F)$  over a wide range of  $V_F$  for several different values of  $V_{in}$ . For  $-1.1$  V  $< V_F < -0.9$  V,  $V_{QW}$  decreases dramatically as  $V_F$  is

made more negative and the constriction formed by the finger gates pinches off. The decrease in  $V_{QW}$  as pinch-off is approached reflects the fact that, as the resistance of the finger constriction increases, an increasingly smaller fraction of  $V_{in}$  will be dropped across the QW itself. From separate measurements of the conductance of the finger-gate constriction (not shown), we have confirmed that the decrease in  $V_{QW}$  at  $V_F \sim -1.1$  V is indeed due to its pinch-off. The working range of our experiment for tunneling spectroscopy therefore corresponds to  $-1.6$  V  $< V_F < -1.1$  V, since the QW itself pinches off near  $V_F \sim -1.6$  V [see the behavior of  $G_{QW}$  in Fig. 1(c)].

In Fig. 1(c), we plot the variation of  $V_{QW}$  on a voltage scale that allows its evolution over the working range of  $V_F$  to be seen in detail. Deep minima in  $V_{QW}$  occur at the transitions between the steps ( $0 \rightarrow 1$ ,  $1 \rightarrow 2$ , and  $2 \rightarrow 3$ ) in  $G_{QW}$ , reminiscent of the behavior in Ref. 4 and reflecting the enhancement of the 1D DoS that occurs at the Fermi level whenever a 1D subband is depopulated. The negative sign of  $V_{QW}$  at these minima may be understood as follows. In the absence of tunneling, there will be no current flow through the QW so that  $V_{QW} = 0$ . When tunneling occurs, however, all of the current injected from the external reservoir must ultimately flow to the grounded reservoir of the QW, while its other reservoir must adjust to a voltage ( $V_1$ ) that ensures this condition satisfied. Consequently, a nonzero value of  $V_{QW}$  should be obtained. If we consider this problem in terms of the flow of electrons associated with the tunnel current, these are injected into the QW from ground and must ultimately flow to the external reservoir. It is well known for ballistic nanostructures, however, that the geometry-induced guiding of carriers can generate voltage drops that are quite different to those that would be expected classically.<sup>17-19</sup> In the present case, ballistic electrons injected into the QW from the grounded reservoir may overshoot the tunnel barrier to the external reservoir and pass directly, instead, to the reservoir at the other end of the wire. This will cause a buildup of negative charge in this reservoir and so will lead to the appearance of a negative  $V_1$  that will continue to grow until it becomes large enough to block the further accumulation of electrons. Thus, the negative value of  $V_{QW}$  in Fig. 1(c) is a direct signature of the tunneling of current into the QW from the external reservoir, which is enhanced whenever a discontinuity in the 1D DoS is close to the Fermi level (conductance steps). Further support for these ideas is provided by the manner in which the main dips in  $V_{QW}$  track the steps in  $G_{QW}$  as  $V_{SG}$  is varied [Fig. 2(a), contour plots in inset]. As  $V_{SG}$  is made more negative, the steps in  $G_{QW}$  shift to less negative  $V_F$ , as indicated by the lower contour in Fig. 2(a). This plots  $dG_{QW}/dV_F$  versus  $V_F$  and  $V_{SG}$ , so that the transitions between conductance plateaus correspond to the local maxima indicated by the dotted lines. The upper contour plots the corresponding variation of the tunneling signal ( $V_{QW}$ ), for the same range of parameters, and clearly shows that the main minima in this signal follow the steps in  $G_{QW}$  very closely (the dotted lines in this contour follow the same variation as in the lower contour plot).

While the origin of the pronounced dips in  $V_{QW}$  in Fig. 1(c) is well understood, there are several other features of our experiment that require further clarification. Figure 2(a)

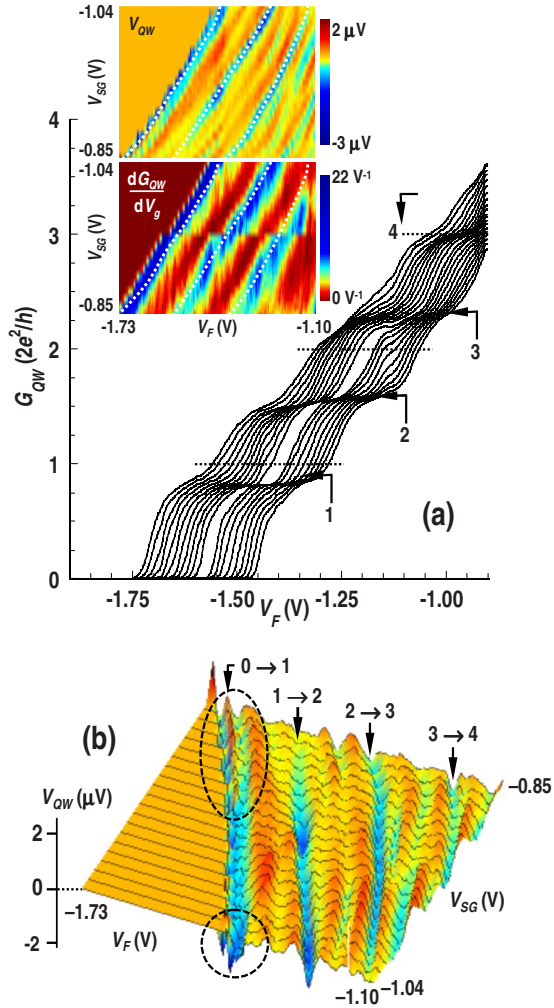


FIG. 2. (Color online) (a) The main plot shows  $G_{QW}(V_F)$  ( $V_{in}=100 \mu\text{V}$ ) as  $V_{SG}$  is incremented in  $-0.1 \text{ V}$  steps between  $-0.85$  and  $-1.04 \text{ V}$  (from left to right, respectively). The contour plots shown in the inset compare the variation of  $V_{QW}$  ( $V_{in}=1 \mu\text{V}$ ) as a function of  $V_F$  and  $V_{SG}$  (upper contour) with that (lower contour) of the transconductance ( $dG_{QW}/dV_F$ , with  $G_{QW}$  in dimensionless units). The dashed lines follow the main dips in  $V_{QW}$  in the upper contour and show that these are correlated with the risers between conductance plateaus (i.e., to regions of large  $dG_{QW}/dV_F$ ). (b) Contour plot of the tunneling signal ( $V_{QW}$ ) for the same experiment of Fig. 2(a). Dotted lines enclose regions where the  $0 \rightarrow 1$  dip shows splitting near the  $0.7$  feature. Temperature:  $0.03 \text{ K}$ .

shows  $G_{QW}(V_F)$  for a number of different values of  $V_{SG}$ , and it is clear from these data that the conductance steps are suppressed below their expected quantized values of integer multiples of  $2e^2/h$ . Nonetheless, the steps appear to be equally spaced, indicating that their values are renormalized by the same factor. This behavior can be explained by considering the influence of electron injection into the external reservoir when current is driven between the source and drain of the QW [as in Fig. 1(a)]. If we ignore for now the role of the external reservoir in our experiment, the quantized conductance of 1D wires arises quite generally since their source and drain reservoirs inject carriers with opposite

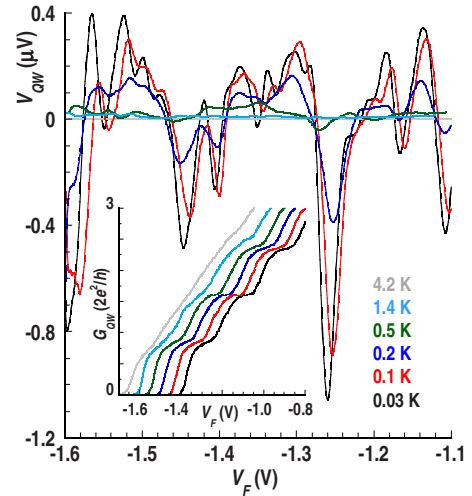


FIG. 3. (Color online) The main panel plots  $V_{QW}(V_F)$  at various temperatures ( $V_{in}=1 \text{ mV}$ ,  $V_{SG}=-0.92 \text{ V}$ , temperatures indicated). The inset shows the corresponding temperature-dependent variation of  $G_{QW}(V_F)$  ( $V_{in}=100 \mu\text{V}$ ). The  $4.2 \text{ K}$  curve is unshifted along the  $V_F$  axis, while the lower-temperature ones are shifted horizontally in successive increments of  $+50 \text{ mV}$ .

momenta, filling the subbands up to separate energies defined by their local electrochemical potentials.<sup>20</sup> Since ballistic carriers injected into such QWs do not undergo any scattering inside it, a distinct identification can therefore be made between the direction of carriers and the reservoir from which they emanated, and it is this property that ultimately leads to the conductance quantization.<sup>20</sup> If we now allow coupling to the external reservoir, although it cannot draw a net current, carriers may be injected into it from the QW before eventually tunneling back (since all current must flow to ground). In this sense, the external reservoir should play the role of the dephasing reservoir proposed by Büttiker,<sup>21</sup> randomizing the phase of injected carriers and reinjecting them into the QW after equilibrating them at its own electrochemical potential. If we consider an extreme situation where *all* carriers injected into the QW tunnel into the external reservoir, the effect would essentially be to break the QW into two shorter wires, each of whose conductance would be quantized in integer units of  $2e^2/h$  but whose total conductance would show steps in units of  $e^2/h$ . In Fig. 2(a), however, the conductance steps are suppressed some  $\sim 15\%$  below their expected values, which indicates an intermediate situation where only a fraction of the carriers in the QW actually tunnel to the external reservoir.

In Fig. 3 (main panel and inset), we compare the temperature dependence of the tunnel-induced voltage ( $V_{QW}$ ) with that of  $G_{QW}$ . This shows that the temperature scale on which the broad dips in  $V_{QW}$  are suppressed is consistent with that on which the steps in  $G_{QW}$  are washed out. This correlation further supports the notion that the broad dips in  $V_{QW}$  are related to the 1D DoS of the QW.

The evolution of the steps in  $G_{QW}$  in a perpendicular magnetic field is shown in Fig. 4(a) and is consistent with the discussion immediately above. As the magnetic field is increased to the relatively modest value of  $500 \text{ mT}$ , Fig. 4(a) shows that the steps in  $G_{QW}$  shift toward the expected integer



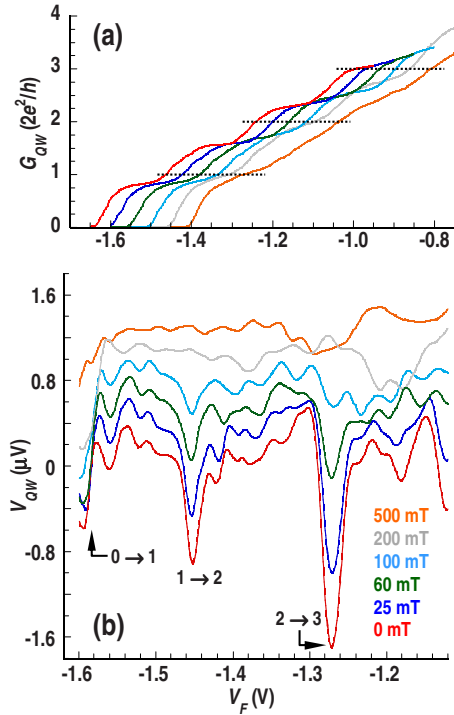


FIG. 4. (Color online) (a)  $G_{QW}(V_F)$  at various magnetic fields [ $V_{in}=100 \mu\text{V}$ ,  $V_{SG}=-0.92 \text{ V}$ , field values indicated in Fig. 4(b)]. Curves for increasing field are shifted horizontally in increments of  $+50 \text{ mV}$ . Dotted lines indicate expected quantized plateaus (at zero magnetic field) in integer units of  $2e^2/h$ . (b)  $V_{QW}(V_F)$  at various magnetic fields ( $V_{in}=1 \text{ mV}$ ). Curves for increasing field are shifted upward in successive increments of  $+0.2 \text{ mV}$ . Temperature in (a) and (b) is  $0.03 \text{ K}$ .

values of  $2e^2/h$  (indicated by the dotted lines). In Fig. 4(b), we show the associated variation of  $V_{QW}$  and see that this tunneling-related signature is strongly suppressed by the magnetic field. This behavior indicates that the magnetic field decreases the tunnel coupling between the external reservoir and the QW, a result that is consistent with the known ability of such a field to lower transmission through a tunnel barrier due to the associated cyclotron-energy cost.<sup>22</sup> Comparing the behavior in Figs. 4(a) and 4(b), we can therefore conclude that the shift of the conductance steps toward the expected integer values of  $2e^2/h$  occurs due to the suppression of tunneling between the QW and the external reservoir, as described in paragraph above.

The final feature of our data we discuss is the reproducible oscillations that we find to be superimposed upon the subband-related dips in  $V_{QW}$ . The oscillations shift systematically as the wire confinement [Fig. 2(b)] or magnetic field [Fig. 4(b)] is varied and can even change the sign of  $V_{QW}$  from negative to positive. They are suppressed with increas-

ing  $V_{in}$  [Fig. 1(c)] and temperature (Fig. 3), all of which features are suggestive of a quantum-interference effect. While conductance resonances due to scattering from impurities or other geometric irregularities have previously been observed in the conductance of QWs,<sup>23,24</sup> it is worth emphasizing that no such structure is present in our direct measurements of  $G_{QW}$  itself [see Fig. 2(a), for example]. This indicates that the oscillatory structure in  $V_{QW}$  is associated with the manner in which the tunnel current is injected into the QW in the spectroscopic geometry of Fig. 1(b). A likely scenario is that, in this configuration, the QW functions as a Fabry-Pérot interferometer, since current injected into the wire may be transmitted into multiple subbands and in both directions along the wire. The quantum interference of these different partial waves should then cause the transmission of carriers along the wire to be modulated by variations of either the QW profile or a magnetic field, just as we observe in our experiment. We emphasize again that this interference mechanism should only be appropriate in the situation where we inject into the QW from the external reservoir. In the geometry of Fig. 1(a), in contrast, carriers are either directly transmitted between the source and the drain or have their phase randomized through injection into the external reservoir, so that no interference behavior is expected.

In conclusion, we have investigated the tunneling into a 1D wire connected to an external reservoir and have shown its tunnel signal to consist of a combination of broad dips, related to the discontinuities in the 1D DoS, and smaller oscillations that are consistent with coherent quantum interference of electron partial waves in the QW. A suppression of the 1D conductance steps below their integer quantized values (in units of  $2e^2/h$ ) has been attributed to the influence of electrons that tunnel back and forth between the QW and the external reservoir. Consistent with this, the QW conductance steps were found to move toward their expected values by applying a magnetic field, which reduces the tunnel coupling between the reservoir and the wire. Interestingly, Fig. 1(c) systematically shows a splitting of the dip corresponding to the  $0 \rightarrow 1$  transition, which appears to be correlated with the 0.7 feature. The splitting is found for many different side-gate voltage conditions [see regions enclosed by dotted lines in Fig. 2(b)], and in future it will be of interest to explore whether it may be used as a probe of the DoS in the region near the 0.7 feature.

This work was supported by the Department of Energy (Grant No. DE-FG03-01ER45920) and was performed, in part, at the Center for Integrated Nanotechnologies, a U.S. DOE, Office of Basic Energy Sciences, Nanoscale Science Research Center. Sandia National Laboratories is a multiprogram laboratory operated by Sandia Corporation, a Lockheed-Martin Co., for the U.S. Department of Energy under Contract No. DE-AC04-94AL85000.

<sup>1</sup>M. Fiske, *Rev. Mod. Phys.* **36**, 221 (1964).

<sup>2</sup>T. Schmidt, R. J. Haug, V. I. Fal'ko, K. v. Klitzing, A. Förster, and H. Lüth, *Phys. Rev. Lett.* **78**, 1540 (1997).

<sup>3</sup>A. K. Geim, P. C. Main, N. La Scala, Jr., L. Eaves, T. J. Foster, P. H. Beton, J. W. Sakai, F. W. Sheard, M. Henini, G. Hill, and M. A. Pate, *Phys. Rev. Lett.* **72**, 2061 (1994).

- <sup>4</sup>C. C. Eugster and J. A. del Alamo, *Phys. Rev. Lett.* **67**, 3586 (1991).
- <sup>5</sup>J. W. Sakai, T. M. Fromhold, P. H. Beton, L. Eaves, M. Henini, P. C. Main, F. W. Sheard, and G. Hill, *Phys. Rev. B* **48**, 5664 (1993).
- <sup>6</sup>P. H. Beton, J. Wang, N. Mori, L. Eaves, P. C. Main, T. J. Foster, and M. Henini, *Phys. Rev. Lett.* **75**, 1996 (1995).
- <sup>7</sup>O. M. Auslaender, A. Yacoby, R. de Picciotto, K. W. Baldwin, L. N. Pfeiffer, and K. W. West, *Phys. Rev. Lett.* **84**, 1764 (2000).
- <sup>8</sup>D. A. Wharam, T. J. Thornton, R. Newbury, M. Pepper, H. Ahmed, J. E. F. Frost, D. G. Hasko, D. C. Peacock, D. A. Ritchie, and G. A. C. Jones, *J. Phys. C* **21**, L209 (1988).
- <sup>9</sup>A. Ramamoorthy, J. P. Bird, and J. L. Reno, *Appl. Phys. Lett.* **89**, 013118 (2006).
- <sup>10</sup>A. Ramamoorthy, J. P. Bird, and J. L. Reno, *Appl. Phys. Lett.* **89**, 153128 (2006).
- <sup>11</sup>A. Ramamoorthy, J. P. Bird, and J. L. Reno, *J. Phys.: Condens. Matter* **19**, 276205 (2007).
- <sup>12</sup>M. Büttiker, *Phys. Rev. B* **41**, 7906 (1990).
- <sup>13</sup>O. E. Raichev and P. Debray, *J. Appl. Phys.* **93**, 5422 (2003).
- <sup>14</sup>K. J. Thomas, J. T. Nicholls, M. Y. Simmons, M. Pepper, D. R. Mace, and D. A. Ritchie, *Phys. Rev. Lett.* **77**, 135 (1996).
- <sup>15</sup>For a recent overview, *J. Phys.: Condens. Matter* **20** (2008), see the special issue on the 0.7 feature that appeared in the April 23rd issue edited by M. Pepper and J. P. Bird.
- <sup>16</sup>K. J. Thomas, J. T. Nicholls, N. J. Appleyard, M. Y. Simmons, M. Pepper, D. R. Mace, W. R. Tribe, and D. A. Ritchie, *Phys. Rev. B* **58**, 4846 (1998).
- <sup>17</sup>M. L. Roukes, A. Scherer, S. J. Allen, H. G. Craighead, R. M. Ruthen, E. D. Beebe, and J. P. Harbison, *Phys. Rev. Lett.* **59**, 3011 (1987).
- <sup>18</sup>C. J. B. Ford, S. Washburn, M. Büttiker, C. M. Knoedler, and J. M. Hong, *Phys. Rev. Lett.* **62**, 2724 (1989).
- <sup>19</sup>T. Kakuta, Y. Takagaki, K. Gamo, S. Namba, S. Takaoka, and K. Murase, *Phys. Rev. B* **43**, 14321 (1991).
- <sup>20</sup>C. W. J. Beenakker and H. van Houten, *Solid State Phys.* **44**, 1 (1991).
- <sup>21</sup>M. Büttiker, *Phys. Rev. B* **33**, 3020 (1986).
- <sup>22</sup>J. P. Bird, K. Ishibashi, M. Stopa, Y. Aoyagi, and T. Sugano, *Phys. Rev. B* **50**, 14983 (1994).
- <sup>23</sup>B. J. van Wees, L. P. Kouwenhoven, E. M. M. Willems, C. J. P. M. Harmans, J. E. Mooij, H. van Houten, C. W. J. Beenakker, J. G. Williamson, and C. T. Foxon, *Phys. Rev. B* **43**, 12431 (1991).
- <sup>24</sup>D. J. Reilly, G. R. Facer, A. S. Dzurak, B. E. Kane, R. G. Clark, P. J. Stiles, J. L. O'Brien, N. E. Lumpkin, L. N. Pfeiffer, and K. W. West, *Phys. Rev. B* **63**, 121311(R) (2001).